

Pulsed RF discharges, glow and filamentary mode at atmospheric pressure in argon

N Balcon^{1,2}, A Aanesland¹ and R Boswell¹

¹ RSPHysSE, Australian National University, Canberra 0200, Australia

² CPAT, Université Paul Sabatier, Toulouse 31000, France

E-mail: nicolas.balcon@anu.edu.au

Received 19 May 2006, in final form 12 December 2006

Published 12 January 2007

Online at stacks.iop.org/PSST/16/217

Abstract

The properties of a pulsed radio frequency capacitive discharge are investigated at atmospheric pressure in argon. The discharge can operate in two different modes: a homogeneous glow discharge or turn into filaments. By pulsing the 13.56 MHz generator both the filamentary and the glow modes can be selected depending on the pulse width and period. For a 5 μ s pulse width (~ 70 RF cycles in the pulse), short pulse periods (less than 100 μ s) result in a filamentary discharge while long pulse periods (greater than 1 ms) result in a glow discharge.

Optical emission spectroscopy and power measurements were performed to estimate the plasma temperature and density. Water vapour was introduced to the discharge as a source of hydrogen and the Stark broadening of the Balmer H_{β} line was measured to allow the plasma density to be estimated as 10^{15} cm⁻³ in the filamentary mode. The estimation of the glow mode density was based on power balance and yielded a density of 5×10^{11} cm⁻³. Emission line ratio measurements coupled with the Saha equation resulted in an estimate of electron temperature of approximately 1.3 eV for the glow mode and 1.7 eV for the filaments.

Using the glow mode at a duty cycle of 10% is effective in decreasing the hydrophobicity of polymer films while keeping the temperature low.

(Some figures in this article are in colour only in the electronic version)

1. Introduction

Atmospheric pressure gas discharges have received an increasing amount of attention over the past ten years, both from academic research groups and from industries wishing to modify the surface properties of materials [1]. The primary reason for this is cost of ownership; atmospheric plasmas do not require large, expensive and power consuming vacuum systems, and they can be operated for on-line surface treatment, for example, in a web to web configuration. The absence of pump down time and vacuum compatibility issues is another factor of cost reduction.

Dielectric barrier discharges (DBD) operating with either sinusoidal signals around 10 KHz or pulsed high voltages, where the dielectric prevents the formation of high temperature

arcs, are the most common atmospheric pressure systems currently in use [2]. At such high pressure, an electron avalanche crossing the gap would have a radial extension (due to diffusion) much smaller than the diameter of the electrodes (typically 10 cm). Consequently, avalanches are unlikely to overlap each other and the discharge usually consists of several filaments. However, under certain conditions, a homogeneous glow mode can be observed. This phenomenon has been classified as the 'one atmosphere uniform glow discharge plasma', OAUGDP [3–5].

Higher frequencies are also used at atmospheric pressure; Moon *et al* recently reported RF glow discharges at atmospheric pressure using a dielectric barrier with a U shape geometry [6]. Park *et al* also reported on an RF glow discharge with bare electrodes [7]. In both the experiments,

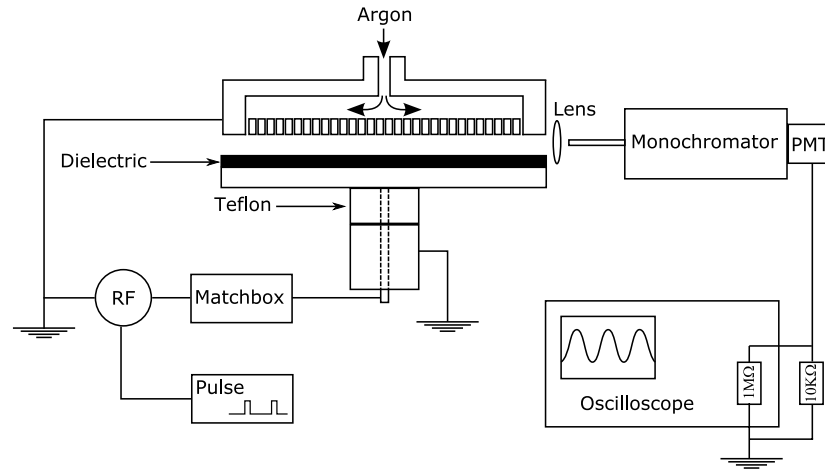


Figure 1. Experimental set-up.

the atmospheric pressure high frequency glow discharge has properties comparable with a lower pressure RF capacitive discharge.

The present experiment operates at 13.56 MHz so that the dielectric can be neglected as an electrical component in the external circuit and the discharge is really a high pressure capacitive discharge where the output capacitor of the RF generator ensures that no direct current can flow [8], (chapter 11, *Capacitive Discharges*). It is more likely that the discharge occurs in the alpha mode rather than in the gamma mode; however a change in the mode could be involved in the transition glow-filament which is not yet well understood.

An advantage of using 13.56 MHz is that the breakdown voltage, which depends on the frequency, is lower in the MHz region [9]. The discharge operates at approximately 76 Torr cm, where the breakdown voltage for a dc discharge is around 3 kV in argon. At 13.56 MHz the breakdown voltage is only 1.4 kV peak to peak [10, 11].

Also, by pulsing the RF signal, it is possible to control the plasma properties and prevent the dielectric from reaching too high a temperature for surface treatment. Plasma diagnostic at atmospheric pressure in narrow gaps is somewhat complicated, therefore time resolved optical emission spectroscopy and power balance were used to measure the evolution of the electron temperature and density in the discharge.

2. Experimental configuration

The atmospheric pressure discharge set-up is shown in figure 1. It consists of two disc parallel electrodes of 10 cm diameter, the distance between them being adjustable up to 5 mm. The top electrode is grounded and feeds the gap with argon via a shower head having an array of one hundred holes, each 0.5 mm in diameter. The argon flow value is 1 standard L/m . The RF power supply (ENI 600 W–13.56 MHz) couples the power to the bottom electrode via a Π -matching network and the voltage applied to this electrode is measured with a Tektronix High voltage probe (ratio 1 : 1000). On the top of this electrode lies a 4 mm thick alumina dielectric layer since this material can resist temperature up to 400 °C whereas glass breaks at much lower temperatures. Filaments tend to remain at the same spots

leading to burn marks on the glass, which eventually breaks. Under certain conditions a glow discharge can be obtained without the dielectric barrier. This would not be possible at frequencies around 10 KHz and it shows that this experiment is similar to a RF capacitive discharge. However, the glow mode without the dielectric barrier is unstable and does not cover the whole electrode area. The use of the dielectric allows the plasma homogeneity to be dramatically improved although the reason for that is not clear at present.

Optical emissions from the plasma are collected with a converging lens and an optical fibre and detected by a monochromator and photomultiplier tube (SPEX-500M, Hamamatsu PMT R777). The total time response of this optical set-up is determined by a 10 K Ω resistor added in parallel with the input channel of the oscilloscope (HP Mega Zoom) yielding an RC rise time of 1 μ s. The RF power supply is controlled by a pulse generator (PM 5715 1 Hz–50 MHz Philips). The pulsed DBD have already been used to make atmospheric pressure discharges more homogeneous [12, 13]. This present experimental set-up aims to test a new method for improving the high pressure surface treatment versatility without risking damage to the polymer specimens.

3. Pulsed discharge

In figure 2 the voltage applied to the DBD and the light emission of the 696.55 nm A I line during a 10 μ s pulse are represented. These measurements were made when the plasma was in a glow mode where the breakdown evolves as a low pressure capacitive discharge. For this experiment, the RF voltage increases to a maximum in less than 1 μ s (time response due to the matchbox) and reaches the breakdown value of 1.4 kV peak to peak. After the ignition of the plasma, the voltage drops to a slightly lower constant value at 2 μ s. The intensity of the 696.55 nm A I line increases rapidly, reaching a maximum after 1 μ s, then drops by over a factor of 5 when the voltage drops to become fairly constant at 2 μ s. This behaviour was observed for all emission lines of the plasma spectrum. The variation of light intensities was measured for 5 lines: A I: 6965.5431 nm, 7503.869 nm and 7723.761 nm and A II: 4131.724 nm and 4277.528 nm.

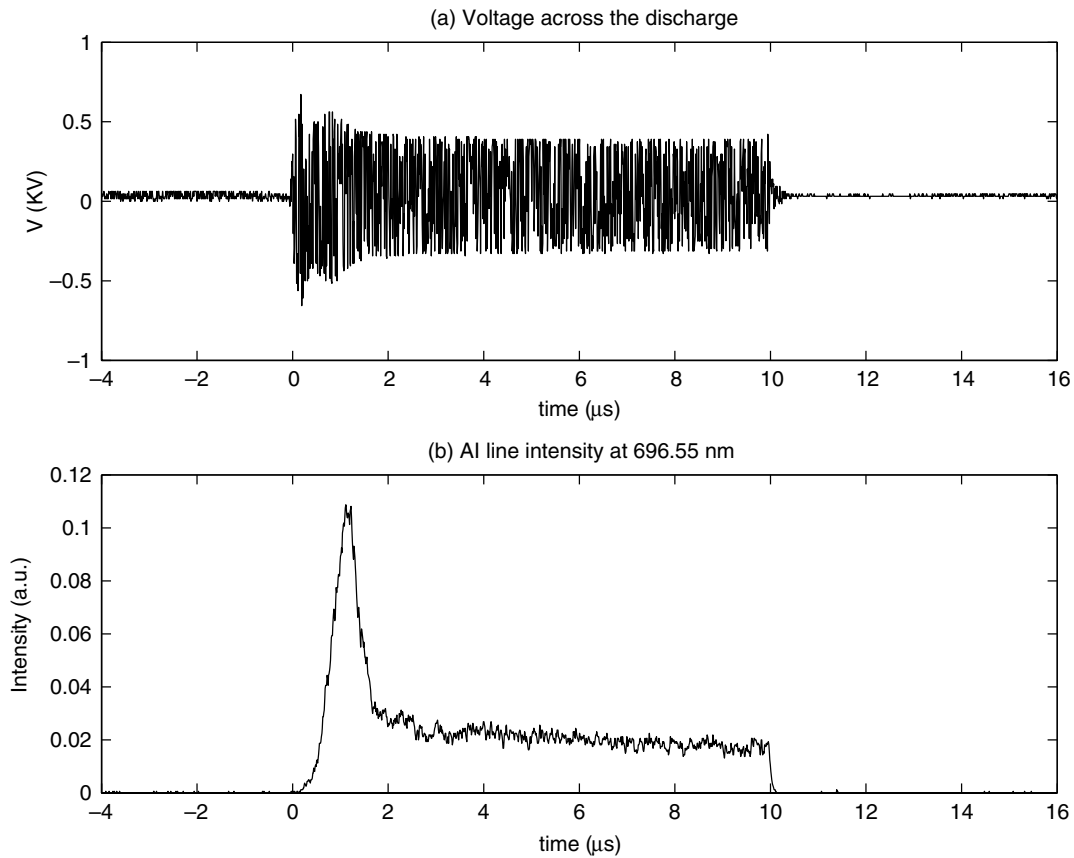


Figure 2. Voltage (a) and line intensity (b).

When the plasma is running in a continuous mode, the voltage across the discharge stays constant at around half the value of the breakdown voltage and the dielectric temperature quickly increases. By pulsing the plasma, the discharge is constantly turned on and off so that the breakdown voltage is reached at the beginning of each pulse and at the same time, the dielectric temperature is kept low, which is interesting for the surface treatment.

In addition, by varying the pulse width and the pulse period it is possible to modify and, in fact, determine the plasma mode; for example, it is possible to force filaments to be created, allowing their formation to be investigated, or to prevent them from appearing and staying in the glow mode. Figure 3 shows two photographs of the plasma in those two different modes: (a) glow and (b) filamentary. Both the modes are obtained with a $5 \mu\text{s}$ pulse width (~ 70 RF cycles in a pulse). With no other parameters being changed, the glow mode is observed when the pulse period is 1 ms or greater and the filamentary mode is obtained when the pulse period is $100 \mu\text{s}$ or less.

Figure 4 shows the areas of existence for the two discharges in a pulse period versus pulse width diagram for an input power of 100 W and a 1 mm gap.

Point 1. For a $5 \mu\text{s}$ pulse width, when the pulse period is $100 \mu\text{s}$, the charges deposited on the dielectric during the previous pulse remain on its surface and when a new pulse occurs, the breakdown is easier at this location (this is known as the memory effect for the DBD). The plasma is turned off between each pulse as demonstrated in figure 2 where the light

intensity drops to zero as soon as the pulse ends. However, once the plasma is in the filamentary mode, the filaments remain at the same location for every pulse.

Transition Point 1 \rightarrow Point 2. When the pulse period is increased and the pulse width is kept constant ($5 \mu\text{s}$, same value as for point 1), the discharge changes from a filamentary mode to a glow mode. This transition is not very sharp and can occur in the opposite direction: glow to filament.

Transition Point 1 \rightarrow Point 3. When the pulse width is increased and the pulse period is kept constant ($100 \mu\text{s}$, same value as for point 1), the discharge changes from a filamentary mode to a glow mode. This also increases the power coupled to the plasma and the temperature. As the previous transition, this transition is not very sharp and can occur in the opposite direction: glow to filament.

When the RF generator is running continuously, both the modes can exist depending not only on all the experimental parameters but also on ambient conditions (pressure, relative humidity and temperature). In addition, for the continuous RF the filament appearance was found to be irreversible and the filament mode more stable than the glow mode. Pulsing the discharge is always efficient in controlling the transition from one mode to the other whatever the ambient conditions are.

For a safe surface treatment, point 2 is of particular interest because it is situated in the glow plasma mode, so the surface treatment is homogeneous, and a long pulse period combined with a short pulse width leads to a low temperature. In section 5

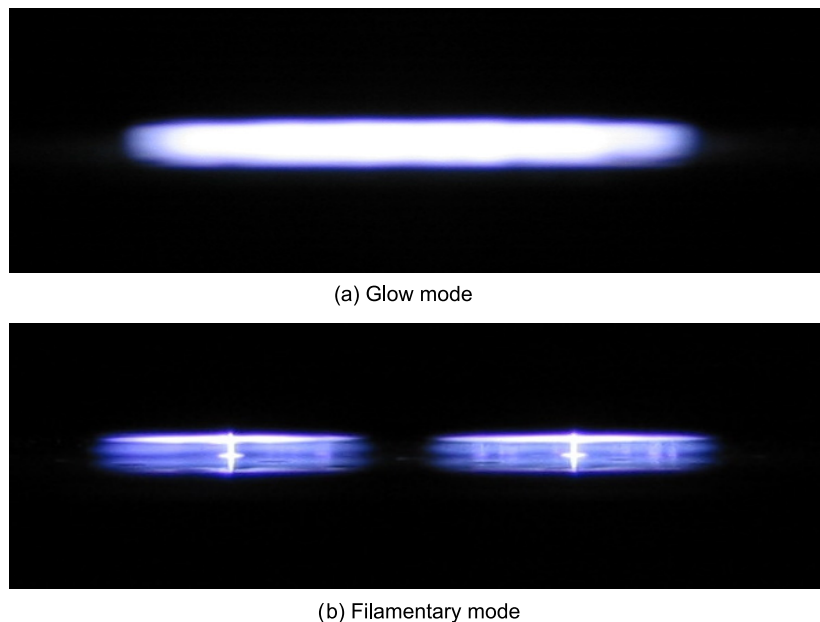


Figure 3. The two different modes.

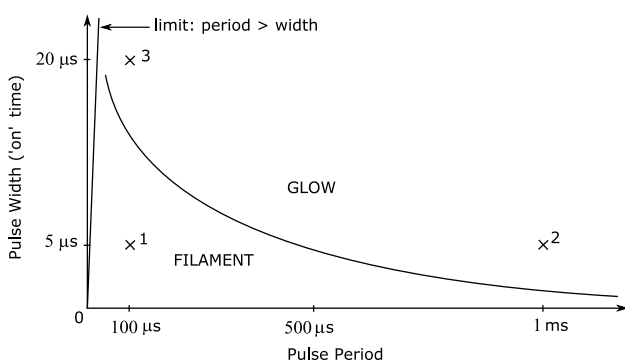


Figure 4. Filament to glow and glow to filament transitions.

the efficiency of this plasma regime for the modification of hydrophobicity is discussed.

4. Temperature and density diagnostic

4.1. Electron density measurement

4.1.1. *Stark broadening method for determining the electron density in the filamentary mode.* Since the electron temperature is determined from the line ratio between different ionization levels, the Saha equation is used where a knowledge of the electron density is necessary; hence a measurement of this important parameter is necessary.

The Stark broadening of the H_{β} line 486.1 nm gives a reasonable approximation of the electron density. In theory the Stark broadening depends on both the electron temperature and density; however for an atmospheric pressure plasma in argon ($10^{11} \leq n_e \leq 10^{17} \text{ cm}^{-3}$) the variation with electron temperature can be neglected [14].

Hydrogen is added to the discharge by dividing the argon line into two: one of pure argon and the other with argon going through a bubbler half full of water, adding water vapour in

Table 1. FWHM for different broadening mechanisms. P is the pressure in atmosphere, T is the gas temperature in kelvin (close to room temperature), χ_H is the mole fraction of hydrogen atoms ($\sim 10\%$) and n_e is electron density in cm^{-3} .

Broadening	FWHM in nm
$\Delta\lambda_{\text{resonance}}$	$60.4 \chi_H (P/T) \simeq 0.02$
$\Delta\lambda_{\text{Van der Waals}}$	$3.6 \times P/T^{0.7} \simeq 0.06$
$\Delta\lambda_{\text{Doppler}}$	$3.48 \times 10^{-4} \sqrt{T} \simeq 0.006$
$\Delta\lambda_{\text{natural}}$	6.2×10^{-5}
$\Delta\lambda_{\text{instrumental}}$	0.19
$\Delta\lambda_{\text{Stark}}$	$2 \times 10^{-11} (n_e)^{2/3}$

the gas line. The flow ratio is controlled by two independent needle valves. Adding water vapour in the plasma disturbs its properties and it was not possible to find the glow mode even though the minimum water vapour possible was added to allow the H_{β} line to be detected in the spectrum background light of other species. Therefore, the Stark broadening method was used as a density diagnostic only for the filamentary mode and the power balance measurement was used for the glow mode.

Table 1 gives the full width at half maximum (FWHM) broadening values for all the mechanisms that may affect the H_{β} line in these conditions.

The openings of the two slits (input of the monochromator and input of the PMT) are set to $60 \mu\text{m}$. With a narrower opening the signal from the H_{β} line is too low to be detected; with a wider opening the instrumental resolution is not sufficiently high and the resulting spectral output would be the sum of several atomic lines rather than the H_{β} line. The calibration of the instrumental function was made with a mercury lamp on the $\text{Hg I } 546.075 \text{ nm}$ line and was found to be a Gaussian of FWHM 1.9 \AA .

Of all the mechanisms independent of the electron density, the instrumental broadening is the largest by one order of magnitude. Thus, only the instrumental and Stark broadenings are used to fit the experimental data and the other mechanisms

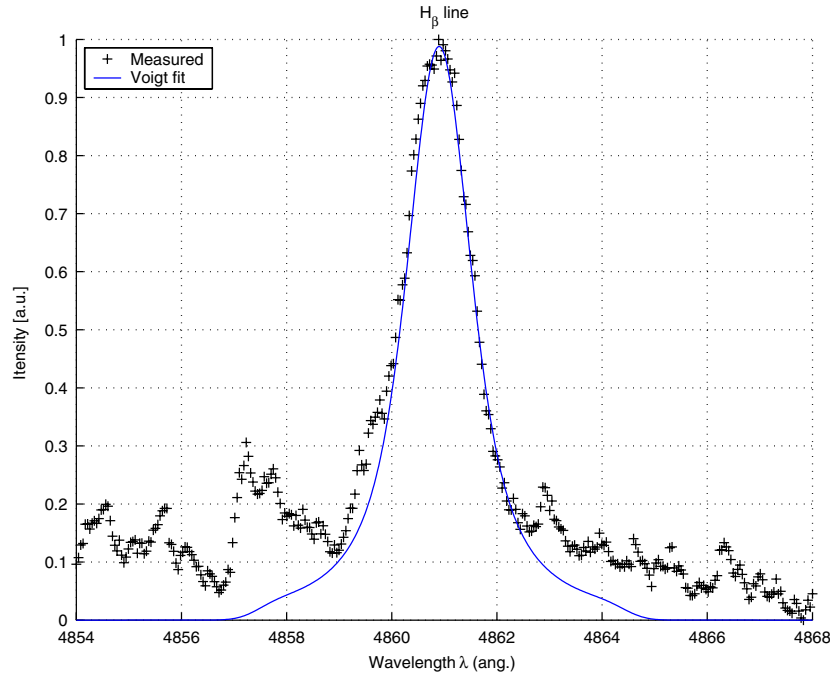


Figure 5. One example of the Voigt fit of H_{β} line.

are neglected. Each broadening mechanism being independent of the others, the combined line profile is the convolution product of the line profiles of each mechanism. The Stark broadening is known to be a Lorentzian function [15], its integral value must be equal to the integral value of the instrumental Gaussian and they must fit the measured H_{β} when convoluted together. Their convolution is a Voigt function. An example of fitting the Voigt profile to the measured line is shown in figure 5. The average FWHM of the Stark broadening for different monochromator settings is 2.2 \AA resulting in an electron density of 10^{15} cm^{-3} (for the filamentary mode). This value concurs with the results obtained by Dong *et al* [16] by Stark broadening on an argon line.

4.1.2. The power balance method for determining the electron density during the glow mode. The glow mode discharge is homogeneously spread over the whole electrode area, so the plasma density can be estimated from a power balance method described in [8] (chapter 3.5, *Energy Loss per Electron-Ion Pair Created*, page 81 and chapter 10.2, *Electropositive Plasma Equilibrium*, page 304). The energy lost by the system per electron-ion pair can be written as

$$E_{\text{lost}} = V_p + E_e + E_{\text{col}},$$

where V_p is the plasma potential (kinetic energy gain by each ion falling down the wall sheath of $\sim 5kT_e$), E_e is the kinetic energy of electrons lost to the wall ($\sim 2kT_e$) and E_{col} represents the collisional energy loss per electron-ion pair created (taking into account the ionization potential, the excitation energy lost per photon in radiation and elastic collisions with neutrals).

E_{lost} depends on T_e , which is expected to be between 1 and 2 eV [17], and under these conditions E_{lost} can be reasonably

approximated to 50 eV for argon. The total power absorbed by a capacitively coupled plasma can be written as

$$P_{\text{abs}} = 2Aen_e v_b E_{\text{lost}},$$

where $2Aen_e v_b$ represents the total current of the discharge over the area $2A$ of the two electrodes ($A = 80 \text{ cm}^2$) and v_b is the Bohm velocity (which equals the ion sound speed, in our conditions $\sim 2 \times 10^5 \text{ cm s}^{-1}$).

Here we are ignoring the large sheath that is formed at low pressures from the self-bias voltage which dominates the power loss for these discharges. The present system is very collisional and it is not clear how the high pressure sheath on the powered electrode would behave, hence we have ignored it for the present estimate. If it is taken into account then the plasma density would need to be about a factor of 3 lower.

The balance between the input power of 200 W from the RF generator (P_{rf}) and the power lost in the plasma leads to

$$n_e = P_{\text{rf}} / (2Ae v_b E_{\text{lost}}),$$

$$n_e \simeq 5.10^{11} \text{ cm}^{-3}.$$

This is about 2000 times less than the electron density in the filamentary mode and is possibly due to the different area of the filamentary discharge compared with the glow discharge. If the same loss mechanism for the glow mode and the filamentary mode is assumed, one would expect the total area covered by the filaments to be $80 \text{ cm}^2 / 2000 = 4 \times 10^{-2} \text{ cm}^2$. From the burn marks left on the polymer film when the discharge was filamentary, the diameter of a single filament is estimated to be approximately 0.1 mm (area of $3.14 \times 10^{-4} \text{ cm}^2$), hence around 130 filaments are expected over the electrode area which is in good agreement with the observation.

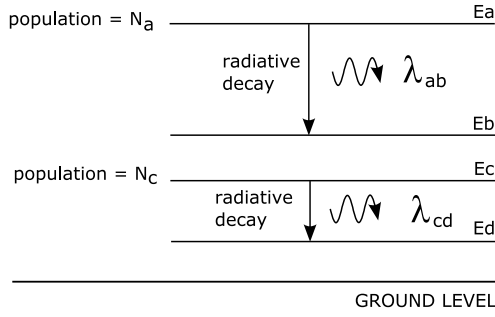


Figure 6. Grotian diagram.

4.2. The Saha–Boltzmann relation for the electron temperature measurement

The average electron density evaluated for the glow and filamentary modes in the previous section is now used to calculate the electron temperature. The use of the Saha equation requires, at least, partial local thermal equilibrium (PLTE) [15]. For the filamentary mode, the system is highly collisional and the electron density around 10^{15} cm^{-3} , so this is not a bad assumption. For the glow mode an assumption of PLTE between the upper levels of each transition is still possible if collisional ionizations and radiative recombinations are supposed to be the dominant processes in the discharge. It is also necessary to assume that the source is optically thin in the direction of observation, which is possibly a poor assumption given the density of the neutral species. However, taking this approximation as the zeroth order, the absolute intensity of the ray corresponding to the transition $a \rightarrow b$ is given by:

$$I_{ab} = \frac{L}{4\pi} hc \frac{A_{ab}N_a}{\lambda_{ab}}, \quad (1)$$

where L is the plasma length along the view axis, h is the Plank constant, c is the celerity of light in vacuum, A_{ab} is the probability of the transition $a \rightarrow b$ (Einstein coefficient), N_a is the population of the upper level of the transition and λ_{ab} is the wavelength of the radiation.

In the PLTE hypothesis, for two transitions $a \rightarrow b$ and $c \rightarrow d$ (figure 6) the Boltzmann distribution relation is

$$\frac{N_a}{N_c} = \frac{g_a}{g_c} e^{(E_c - E_a)/kT_e}, \quad (2)$$

where k is the Boltzmann constant, T_e is the electron temperature, N_c is the population of the upper level of the transition $c \rightarrow d$, g_a and g_c are the statistical weights of levels a and c and E_a and E_c are the energies of the levels a and c .

This equation can be arranged so that the density of the species excited to the level a can be written as

$$N_a = \frac{N}{Z} g_a e^{-E_a/kT_e}, \quad (3)$$

where N is the density of neutral argon and Z the canonical partition function. Equations (1) and (3) yield

$$I_{ab} = \frac{L}{4\pi} hc \frac{N}{Z} \frac{A_{ab}g_a}{\lambda_{ab}} e^{-E_a/kT_e}.$$

The plot of $\ln(I\lambda/gA)$, as a function of E_a for each A II line, gives points which would be perfectly aligned in the case

of a plasma in total thermal equilibrium. The slope of this line is $-1/kT_e$ leading to T_e .

This method (due to Boltzmann) was tested on an inductively coupled plasma of fairly well-known parameters where it is possible to decrease the pressure to check how the electron temperature would vary.

The Boltzmann plots for the 7 and 150 mTorr in the ICP lead to temperatures in agreement within 25% with the Langmuir probe measurements. As expected, the electron temperature decreases when the pressure increases.

This Boltzmann plot method is very sensitive to the ratio between kT_e and the upper levels energy values of the transitions. When it was applied to the A II lines seen in the atmospheric pressure capacitive discharge, the energy spread of the upper levels of A II was too small compared with kT_e and the results were not realistic.

To obtain a higher accuracy, it is necessary to compare the line intensities between different ionization degrees of argon. Then there is at least the ionization potential difference between the A I and A II line intensities. The comparison between neutrals and ions requires the use of the Saha equation:

$$\frac{n_e N_+}{N_n} = 2 \frac{g_+}{g_n} \left[\frac{2\pi m_e k T_e}{h^2} \right]^{3/2} e^{-(E_a - E_c + E_i)/kT_e}, \quad (4)$$

where E_i is the ionization potential of argon, N_n is the population of the upper level of a given transition $a \rightarrow b$ of neutral argon (A I line) and N_+ of the transition $c \rightarrow d$ of ionized argon (A II line) and g_n and g_+ are the statistical weights of levels a (neutral) and c (ionized), respectively.

Coupling equation (1) and (4) leads to

$$\frac{I_+}{I_n} = \frac{2 \lambda_n A_+ g_+}{n_e \lambda_+ A_n g_n} \left[\frac{2\pi m_e k T_e}{h^2} \right]^{3/2} e^{-(E_a - E_c + E_i)/kT_e}, \quad (5)$$

where I_n is the intensity of the A I line (transition $a \rightarrow b$), I_+ is the intensity of the A II line (transition $c \rightarrow d$) and λ_n , λ_+ , A_n and A_+ are the wavelengths and probabilities of the transitions.

In equation (5), the temperature dependence of the intensities ratio is not only in the exponential but also in the factor $(kT_e)^{3/2}$, hence it is impossible to use a graph based averaging of the temperature as done with a classic Boltzmann plot.

However, the electron temperature from several A II/A I ratios can be found from equation (5). Three A I lines and two A II lines will give six A I–A II intensity ratios, each of these ratios giving a temperature.

Figure 7 is an example representing the logarithm of the A II₄₁₃₁/A I₇₇₂₃ ratio as a function of T_e for a plasma density of $n_e = 5 \times 10^{11} \text{ cm}^{-3}$ (glow mode). The cross-over point between the curve $\ln(I_+/I_n)$ and the line representing the measured ratio yields the electron temperature. Six A I–A II combinations for the Saha equation lead to six temperatures which are found to be very close: only 5% variation between them, proving that the plasma is close to PLTE. An average is taken and the temporal evolution is observed during a 10 μs pulse width as represented in figure 8.

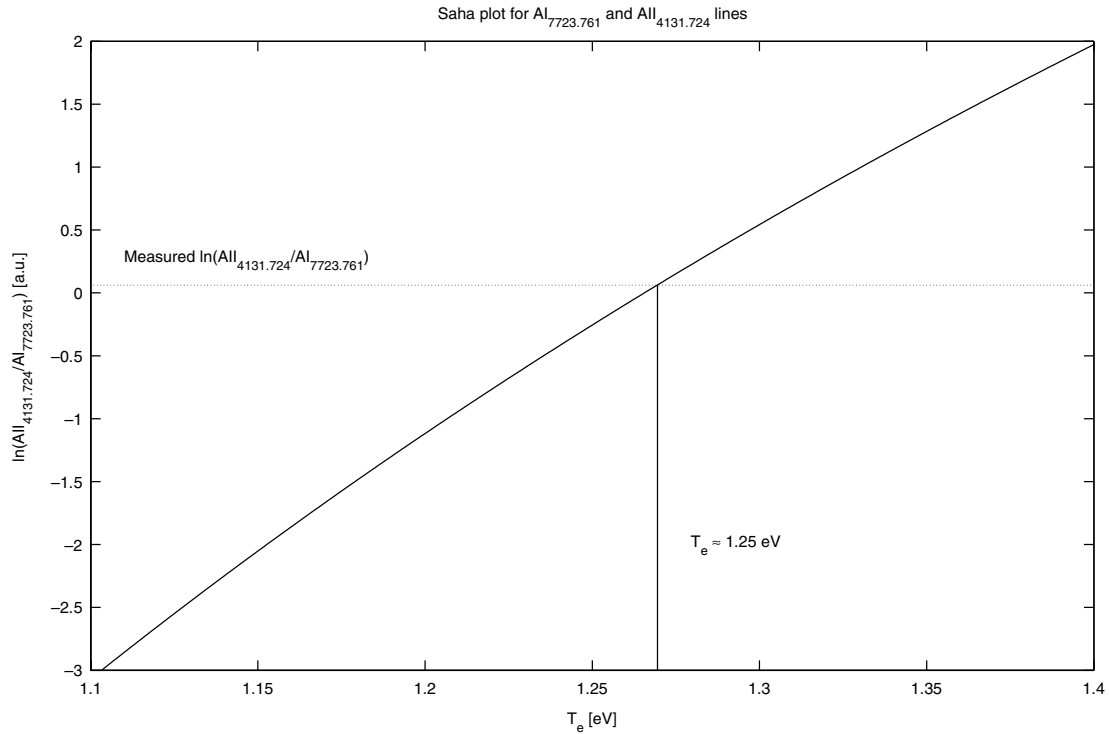


Figure 7. Example of A_{II}/A_I ratio as a function of T_e .

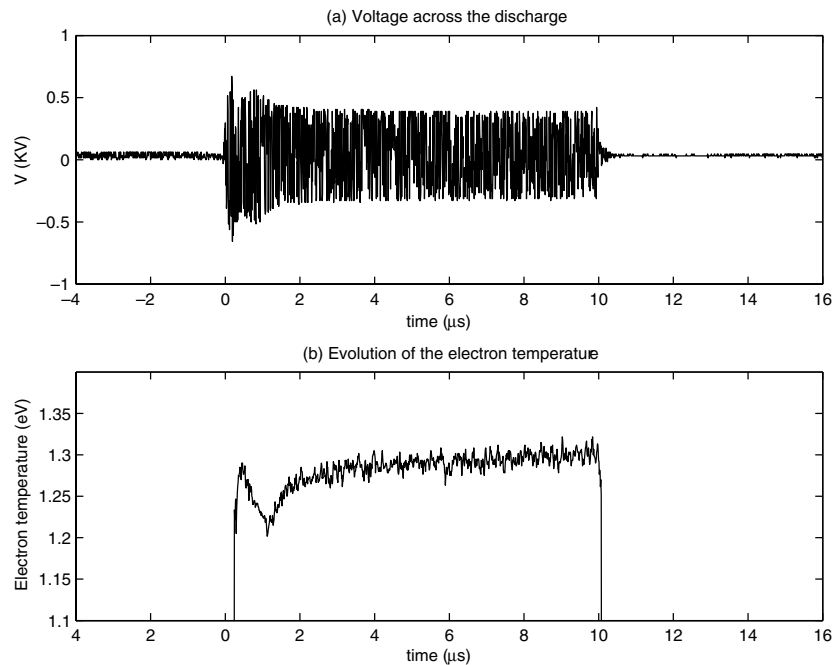


Figure 8. Electron temperature during a pulse in the glow mode.

For the same pulse, the intensity of all argon lines (the 696.5 nm line is represented in figure 2) starts with a peak at the beginning of the pulse and then decreases to reach a plateau as the voltage drops. The electron temperature starts with a peak as well and decreases just after the voltage drops. Then, unlike the light intensity, it slowly increases to reach a plateau of greater value than the initial temperature even when the voltage stays constant at a lower value.

The measurement of the electron density from the Stark broadening and power balance are not time resolved but averaged over time, hence the density values used in the Saha equation are constant over a pulse width. This is probably not very realistic and affects the temperature evolution since its calculation is based on the electron density. However, the average value of an electron temperature between 1.2 and 1.3 eV for the glow mode is reliable.

A similar curve is obtained for the electron temperature in the filamentary mode but with a greater value varying between 1.5 and 2 eV.

5. Surface treatment

Atmospheric pressure surface treatment has been studied in DBDs at 10 KHz [18, 19] and in 13.56 MHz capacitive discharges [6]. In both the cases the treatment increases the wettability of the polymer. The pulsed RF discharge described in section 3 is efficient for the treatment of polyethylene terephthalate (PET) polymer films. By pulsing the RF signal it is possible to reduce the temperature of the polymer by a factor of 3

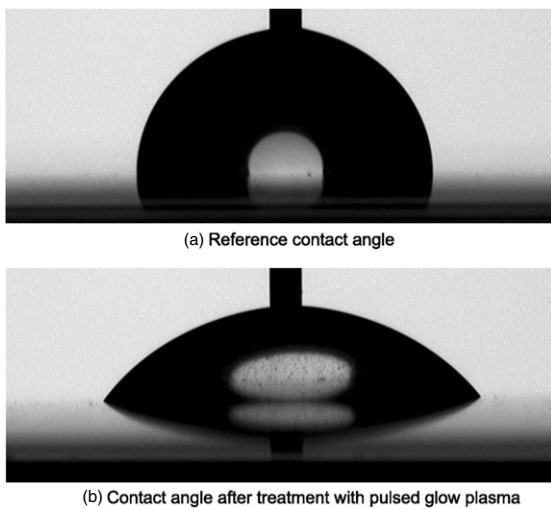


Figure 9. Contact angle with untreated (a) and treated polymer film (b).

compared with a continuous mode. With a continuous RF discharge the electrode and the dielectric quickly reach a temperature of 220 °C, which may cause severe damage to the polymer.

With a 100 μs pulse width and a pulse period of 1 ms (Duty cycle = 10%) the temperature remains below 80 °C and the discharge is prevented from turning into a filament. Were the plasma to become filamentary, a non-uniform surface treatment would result and the polymer may well become burnt on each filament spot.

In figures 9(a) and (b) the contact angle measurement of a droplet of de-ionized water on untreated and treated polymer is shown. An increase in the hydrophilic behaviour of the polymer can be observed: the untreated contact angle of the polymer sample is 90 ° and after one minute exposure in the discharge (pulsed glow mode) the contact angle decreases to 53 °.

Figure 10(a) shows the evolution of the contact angle as a function of the exposure time in the reactor (pulsed glow mode), reaching a plateau at 60 s. The same curve is obtained with a continuous plasma, proving that the surface treatment with a pulsed discharge is as efficient as the continuous mode.

Figure 10(b) shows that the surface modification is durable for a number of days (around two months before recovering the original hydrophobicity level).

6. Conclusion

The experimental results presented in this paper show that an RF non-thermal plasma can be obtained at atmospheric pressure in an argon atmospheric pressure system. Plasma diagnostic at such high pressure is often complicated due to the small gap size and the fast evolution of the plasma parameters. However we have shown that a good estimation of both the electron temperature and density is possible with optical

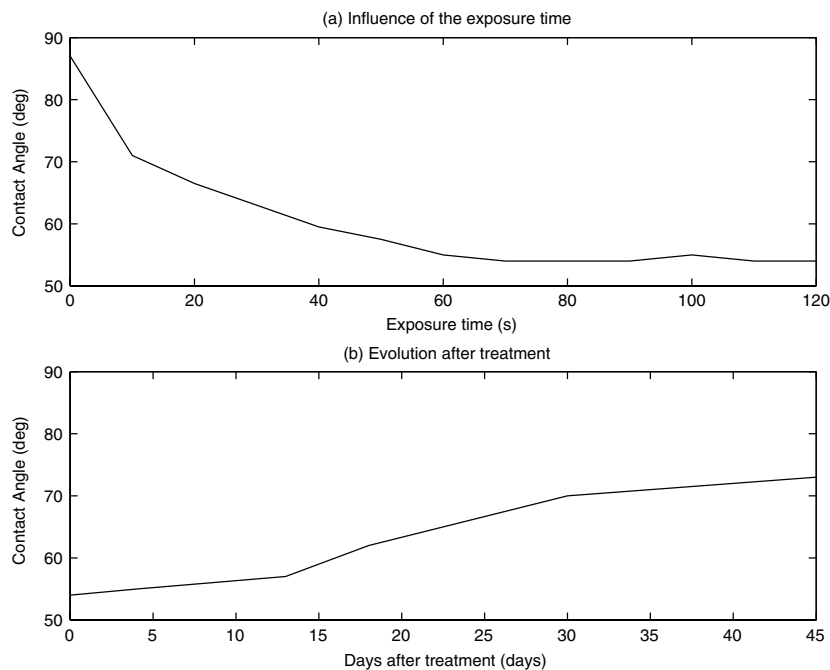


Figure 10. Contact angle as a function of exposure time (a) and days after treatment (b).

emission spectroscopy. This high frequency discharge at atmospheric pressure showed properties comparable to the classic capacitive RF discharge at lower pressure (scaled up with a wider gap). It is stable, and the glow mode is easy to obtain.

Since the discharge runs at atmospheric pressure, and does not require any kind of chamber, it can be used for fast on-line surface treatment of polymers without vacuum compatibility problems. With an appropriate pulse width and period it is possible to have control over the plasma mode and to reduce the temperature in the discharge making it safer for the surface treatment of polymer.

References

- [1] Kogelschatz U 2003 Dielectric-barrier discharges: their history, discharge physics, and industrial applications *Plasma Chem. Plasma Process.* **23** 0272–4324
- [2] Kogelschatz U, Eliasson B and Egli W 1999 From ozone generators to flat television screens: history and future potential of dielectric-barrier discharges *Pure Appl. Chem.* **71** 1819
- [3] Roth J R, Rahel J, Dai X and Sherman D M 2005 The physics and phenomenology of one atmosphere uniform glow discharge plasma (ouagd) reactors for surface treatment applications *J. Phys. D: Appl. Phys.* **38** 555–67
- [4] Massines F, Rabehi A, Decomps P, Gadri R B, Ségur P and Mayoux C 1998 Experimental and theoretical study of a glow discharge at atmospheric pressure controlled by dielectric barrier *J. Appl. Phys.* **83** 2950
- [5] Gherardi N and Massines F 2001 Mechanisms controlling the transition from glow silent discharge to streamer discharge in nitrogen *IEEE Trans. Plasma Sci.* **29** 536
- [6] Moon S Y, Choe W and Kang B K 2003 A uniform glow discharge plasma source at atmospheric pressure *Appl. Phys. Lett.* **84** 188
- [7] Park J, Henins I, Herrmann H W, Selwyn G S, Jeong J Y, Hicks R F, Shim D and Chang C S 2000 An atmospheric pressure plasma source *Appl. Phys. Lett.* **76** 288
- [8] Lieberman M A and Lichtenberg A J 1994 *Principles of Plasma Discharges and Material Processing* (New York: Wiley)
- [9] Smith H B, Charles C and Boswell R W 2003 Breakdown behavior in radio-frequency argon discharges *Phys. Plasmas* **10** 875
- [10] Schütze A 1998 The atmospheric-pressure plasma jet: a review and comparison to other plasma sources *IEEE Trans. Plasma Sci.* **26** 1685
- [11] Kunhardt E E 2000 Generation of large-volume, atmospheric-pressure, nonequilibrium plasmas *IEEE Trans. Plasma Sci.* **28** 189
- [12] Carman R J, Falconer I S and Mildren R P 2005 Dynamics of a homogeneous dielectric barrier discharge in xenon excited by short-voltage pulses *IEEE Trans. Plasma Sci.* **33** 3813
- [13] Mildren R P and Carman R J 2001 Enhanced performance of a dielectric barrier discharge lamp using short-pulsed excitation *J. Phys. D: Appl. Phys.* **34** 3727
- [14] Gigosoy M A and Cardenoso V 1996 New plasma diagnosis tables of hydrogen stark broadening including ion dynamics *J. Phys. B: At. Mol. Opt. Phys.* **29** 4795–838
- [15] Griem H R 1997 *Principles of Plasma Spectroscopy (Cambridge Monographs on Plasma Physics)* (Cambridge: Cambridge University Press)
- [16] Dong L, Ran J and Mao Z 2005 Direct measurement of electron density in microdischarge at atmospheric pressure by stark broadening *Appl. Phys. Lett.* **86** 161501
- [17] Park J, Henins I, Herrmann H W, Selwyn G S and Hicks R F 2001 Discharge phenomena of an atmospheric pressure radio-frequency capacitive plasma source *J. Appl. Phys.* **89** 20
- [18] Massines F and Gouda G 1998 A comparison of polypropylene-surface treatment by filamentary, homogeneous and glow discharges in helium at atmospheric pressure *J. Phys. D: Appl. Phys.* **31** 3411
- [19] Massines F, Messaoudi R and Mayoux C 1998 Comparison between air filamentary and helium glow dielectric barrier discharges for the polypropylene surface treatment *Plasmas Polym.* **3** 43